Journal of Applied Electrochemistry **33**: 37–42, 2003.

Corrosion behaviour of tantalum in sodium hydroxide solutions

A. ROBIN
Departamento de Engenharia de Materiais, Faculdade de Engenharia Química de Lorena, Polo Urbo-Industrial, Gleba AI-6, 12600-000 Lorena, SP, Brazil
(e-mail: alain@demar.faenquil.br)

Received 8 June 2002; accepted in revised form 15 October 2002

Key words: corrosion, passivation, sodium hydroxide, tantalum

Abstract

The corrosion behaviour of tantalum has been investigated in sodium hydroxide solutions at different temperatures, using open-circuit potential measurements, potentiodynamic polarization, polarization resistance method and electrochemical impedance spectroscopy. Tantalum showed a passive behaviour in 5 and 10 wt % NaOH at 25, 50 and 75 °C, and in 15 wt % NaOH at 25 and 50 °C. In 15 wt % NaOH at 75 °C and in 30 wt % NaOH at all temperatures, tantalum presented a passive–active transition (self-activation) due to the spontaneous dissolution of its superficial air-formed oxide, and afterwards remained in the active state for long times, forming a polytantalate compound. In all cases, the corrosion rates increase with increasing NaOH concentration and temperature.

1. Introduction

Tantalum (Ta) has excellent corrosion resistance in most mineral acids, even concentrated and hot, except in hydrofluoric acid [1–8]. This corrosion resistance and inertness of Ta are attributed to a thin protective oxide film, Ta_2O_5, that forms spontaneously in air and that presents a high stability in a variety of aqueous solutions. Because of the wide range of type, concentration and temperature of the acidic media to which it is resistant, Ta has found applications as a material of construction in the chemical-processing industry for heaters, heat exchangers, reaction vessels and impellers for pumps [8–10].

It is known that Ta is attacked, even at room temperature, by concentrated alkaline solutions, but is fairly resistant to dilute alkaline solutions [1]. Whereas some work on the electrochemical properties of Ta and its oxides in acid media are available [11–17], data on the behaviour in alkaline media are very limited [11, 17–18].

The purpose of this work is to study the electrochemical behavior of Ta in sodium hydroxide (NaOH) solutions at different concentrations and temperatures. This investigation is based on open-circuit, potentiodynamic and electrochemical impedance measurements.

2. Experimental procedure

A Ta ingot was obtained by melting of CP–Ta scraps in a 300 kW electron beam furnace (Leybold-Heraeus, ES-2/18/300) using a water-cooled copper crucible under high-vacuum ($<10^{-3}$ Pa). Chemical composition was determined in an inductively coupled plasma spectrophotometer (ARL, model 3410) and gas analyses were carried out by means of the sample melting and inert gas carrier technique (Leco Co., TC-136). The chemical composition of Ta ingot is shown in Table 1.

Ta specimens were prepared from transverse slices cut from the electron beam melted ingot. Cylindrical test specimens (8 mm dia. × 15 mm length) were obtained from these slices and mounted in PTFE holders. The cross-section of the electrodes (0.5 cm^2 area) was mechanically ground with emery-paper up to 600 grit, degreased with acetone, rinsed with distilled water and dried with air.

The solutions, prepared from analytical reagents and de-ionized water, were 5, 10, 15 and 30 wt % NaOH. The solutions were naturally aerated and no stirring was used during the experiments. The temperature of the solutions was maintained at 25, 50 and 75 ± 2 °C. The counter electrode was a square-shaped platinum sheet of 18 cm^2 area. All potentials were referred to the saturated calomel electrode (SCE) potential (+0.242 V vs SHE).

E/t and polarization measurements were performed using a PAR 273A potentiostat controlled with a microcomputer through M352 corrosion software. The electrochemical impedance spectroscopy (EIS) measurements were carried out at open-circuit potentials using an electrochemical interface (Solartron, model 1287A) and a frequency response analyser (Solartron, model 1260A), controlled by a microcomputer through E_{corr}/Z_{plot} (Solartron, model 125587S) software.

Table 1. Chemical composition of Ta

Element	W	Fe	Al	Si	O	N
wt-ppm	<55	<45	<30	<50	64 ± 16	5 ± 3

Prior to cathodic and anodic polarization, the working electrodes were immersed in the solutions for nearly 3 h for stabilization of the open-circuit potential, taking the immersion moment as zero time. The polarization studies were carried out potentiodynamically with 1 mV s^{-1} potential sweep rate. After each polarization experiment, the samples were reground with emery papers to a 600 grit finish to remove any product formed on the metal surface which could affect the following tests, rinsed with distilled water, dried and transferred quickly in the NaOH solution. The impedance measurements were made at open-circuit potential using a sinusoidal signal of 10 mV amplitude and frequencies in the 0.1 Hz–100 kHz range.

Some immersion tests were performed in 15 and 30 wt % NaOH solutions at room temperature and the Ta coupons were observed by scanning electron microscopy (LEO VP-1450 SEM) and analysed using energy-dispersive spectroscopy (EDS) and X-ray diffractometry.

3. Results and discussion

Figure 1 presents the evolution of the open-circuit potential (OCP) of Ta as a function of exposure time in 5 to 30 wt % NaOH solutions at room temperature. Two distinct behaviours are noted depending on NaOH concentration:

(i) The OCP shifts in the positive direction with time. The continuous increase of OCP is associated with the thickening of the air-formed native oxide and suggests that this oxide is resistant to dissolution and that Ta is passive at OCP. This behaviour was observed in 5, 10 and 15 wt % NaOH at room temperature (Figure 1) and 50 °C, and in 5 and 10 wt % NaOH at 75 °C.

(ii) The OCP drops in the negative direction and tends to stabilize for long exposure times. The decrease of OCP with time is indicative of the dissolution of the protective air-formed oxide and the subsequent surface activation. This behaviour was observed in 15 wt % NaOH at 75 °C and in 30 wt % NaOH at 25 °C (Figure 1), 50 and 75 °C. The steady state potentials are in the −1.5 to −1.4 V vs SCE range and are close to the values reported for anodized Ta in 10 M NaOH (~29 wt %) at room temperature after self-activation, nearly −1.44 V vs SCE [18]. In 30 wt % NaOH. the induction time for activation (time required for Ta to exhibit the lowest OCP values) decreased as the temperature increased. The induction times measured at 25, 50 and 75 °C were nearly 1800, 500 and 30 s, respectively.

Figure 2 shows the variation of the corrosion potential (OCP value measured for the longest exposure times) as a function of log (NaOH concentration) and temperature, The corrosion potential shifts in the negative direction as the NaOH concentration increases. Very similar results were obtained for niobium in NaOH solutions at 30 °C [19]. Little difference is noted between the corrosion potentials measured at 25 and 50 °C.

Figure 3 shows the polarization curves of Ta obtained in 5 wt % NaOH solutions at different temperatures. The shape of the curves changes very little with temperature, suggesting that the reactions at the metal–solution interface are the same. Nevertheless, an increase in both cathodic and anodic current densities is observed as the temperature increases. No active–passive transition is observed on the anodic part of the polarization curves, which confirms the passive behaviour of Ta under these conditions, pointed out from the OCP measurements. Similar observations were made for the polarization curves obtained in 10 wt % NaOH, but the current densities are higher for 10 wt % NaOH than for 5 wt % NaOH at the same temperatures.

In 15 wt % NaOH solutions, two kinds of polarization curves were obtained (Figure 4). At 25 and 50 °C, the shape of the curves is very similar to that obtained in 5 wt % (Figure 3) and 10 wt % NaOH, which suggests

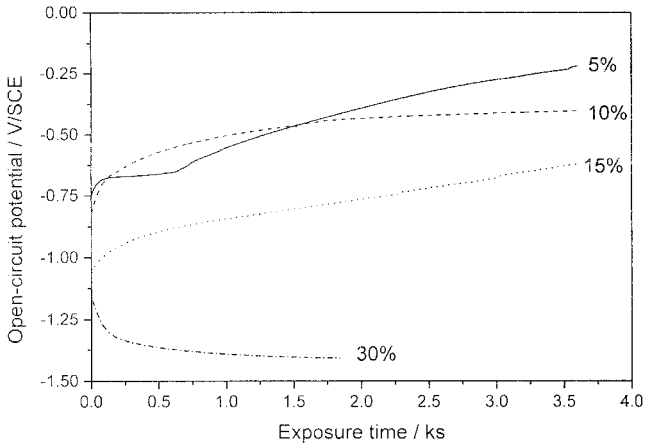

Fig. 1. Variation of open-circuit potential of Ta in NaOH solutions at 25 °C as a function of exposure time.

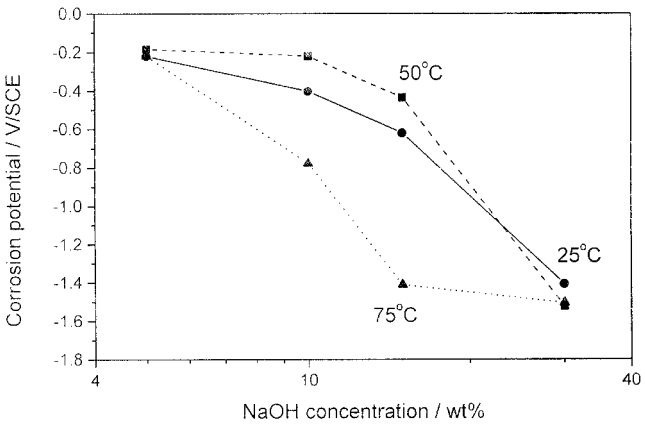

Fig. 2. Variation of corrosion potential of Ta as a function of NaOH concentration and temperature.

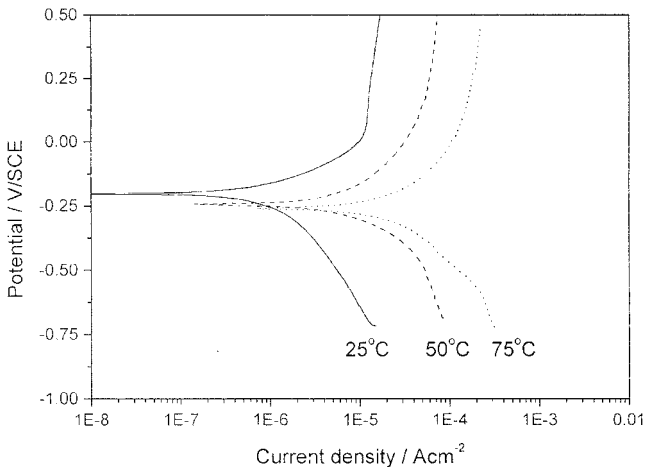

Fig. 3. Anodic and cathodic polarization curves of Ta in 5 wt % NaOH solutions at different temperatures.

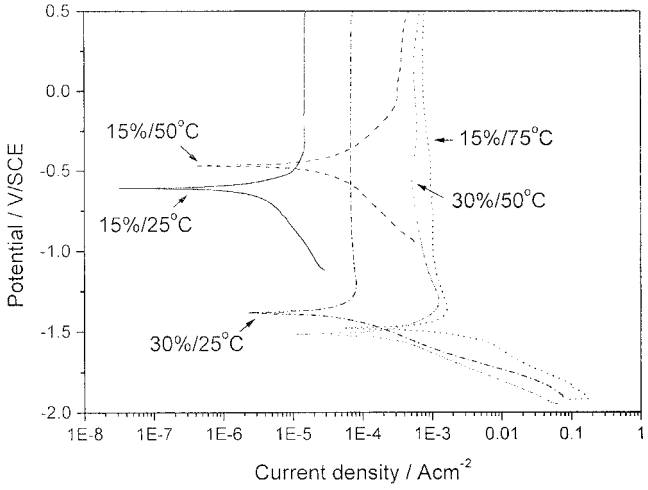

Fig. 4. Anodic and cathodic polarization curves of Ta in 15 and 30 wt % NaOH solutions at different temperatures.

that the same reactions are taking place on the metal surface. The current density increases to some extent as NaOH concentration and temperature increase. No active–passive transition is also noted on the anodic part of the polarization curves.

The curve obtained in 15 wt % NaOH at 75 °C is very different. The slope of the cathodic curve is lower than that observed for the other conditions, which shows that the cathodic reaction is different. The anodic curve presents a current peak, characteristic of an active–passive transition, followed by a passive region. This confirms the active behaviour of Ta in 15 wt % NaOH at 75 °C at OCP, observed from the OCP measurements.

In 30 wt % NaOH solutions, the shape of the cathodic curves is the same for the three temperatures and very similar to that obtained in 15 wt % NaOH at 75 °C (Figure 4), suggesting that the same cathodic reaction occurs at the metal–solution interface, but with a higher rate as NaOH concentration and temperature increase. The anodic polarization curves also present an active–passive transition for all temperatures, and the critical current density increases with increase in temperature.

The main cathodic reactions in aqueous solutions at high pH are the reduction of dissolved oxygen and direct reduction of water, the latter causing hydrogen evolution. At pH close to 14, the equilibrium potentials for the H_2O/O_2 and H_2/H_2O systems are +0.404 V vs SHE (or +0.162 V vs SCE) and −0.826 V vs SHE (or −1.068 V vs SCE), respectively.

Considering that the OPC values for Ta in 5, 10 and 15 wt % NaOH at 25 and 50 °C and in 5 and 10 wt % NaOH at 75 °C are in the −0.8 to −0.2 V vs SCE range (Figure 2), the cathodic reaction taking place at the metal surface is

$$O_2 + 2H_2O + 4e^- \rightarrow 4OH^- \quad (1)$$

In 15 wt % NaOH at 75 °C and in 30 wt % NaOH at 25, 50 and 75 °C, the OCP values range from −1.5 to −1.4 V vs SCE (Figure 2). Thus, the cathodic reaction that dominates under these conditions is

$$2H_2O + 2e^- \rightarrow H_2 + 2OH^- \quad (2)$$

The evolution of gaseous products observed during immersion of Ta samples in 30 wt % NaOH at room temperature corroborates the occurrence of this reaction.

The cathodic slopes are found to be −0.160 and −0.180 V (decade)$^{-1}$ in 30 wt % NaOH at 25 and 50 °C and −0.210 V (decade)$^{-1}$ in 15 and 30 wt % NaOH at 75 °C, which are higher than the reported values for H_2 evolution on tantalum in H_2SO_4 solutions (−0.120 and −0.140 V (decade)$^{-1}$ at 25 and 65 °C, respectively) [20].

The Pourbaix diagram of the Ta–H_2O system does not consider the tantalate and pertantalate species, due to the lack of thermodynamic data, but suggests that these compounds can be formed in high pH solutions [21]. It is reported that in NaOH solutions, the orthotantalate ion, TaO_4^{3-}, is not stable and undergoes hydrolysis, forming the metatantalate ion, TaO_3^-. These ions polymerize to produce isopolytantalate ions, $Ta_6O_{19}^{8-}$ [22].

In 5, 10 and 15 wt % NaOH at 25 and 50 °C and in 5 and 10 wt % NaOH at 75 °C, where Ta is passive, the anodic reaction may occur through oxide formation, according to the following:

$$2Ta + 10OH^- \rightarrow Ta_2O_5 + 5H_2O + 10e^- \quad \text{(anodic film formation)} \quad (3)$$

The blue coloured surface of Ta coupons immersed in 15 wt % NaOH at 25 °C for 500 h corroborates the presence of an oxide film. The partial dissolution of this oxide film and precipitation of isopolytantalate compounds may also occur:

$$3Ta_2O_5 + 8NaOH \rightarrow Na_8Ta_6O_{19} + 4H_2O \quad \text{(dissolution – precipitation)} \quad (4)$$

but $Na_8Ta_6O_{19}$ was not detected by EDS and X-ray diffractometry.

In 15 wt % NaOH at 75 °C and in 30 wt % NaOH at 25, 50 and 75 °C, where Ta undergoes active dissolution, the reactions may be the spontaneous dissolution of air-formed tantalum oxide during OCP drop:

$$3Ta_2O_5 + 8NaOH \rightarrow Na_8Ta_6O_{19} + 4H_2O \quad \text{(air-formed oxide dissolution)} \quad (5)$$

followed by dissolution of Ta base metal and precipitation of isopolytantalate at steady state potential (−1.5 to −1.4 V vs SCE):

$$6Ta + 8NaOH + 30OH^- \rightarrow Na_8Ta_6O_{19} + 19H_2O + 30e^- \quad \text{(dissolution – precipitation)} \quad (6)$$

Gad-Allah [18] proposed similar reactions for dissolution of anodized Ta in NaOH solutions but suggested the formation of the $NaTaO_3$ insoluble product instead of $Na_8Ta_6O_{19}$. The same author proposed the formation of $Na_8Nb_6O_{19}$ for the dissolution of anodized Nb in NaOH solutions [23].

Ta coupons after immersion in 30 wt % NaOH at 25 °C for 54 h were covered by a white powdery corrosion product. Figure 5(a) shows that this product is highly porous and consists of fine crystals. EDS spectrum of the Ta surface reveals the presence of the Na, O and Ta elements (Figure 5(b)). X-ray diffraction pattern shows the characteristic peaks of metallic Ta and a set of well defined peaks at 2Θ lower than 45° (Figure 5(c)). These peaks correspond to the $Na_8Ta_6O_{19}$ compound according to the JCPDS diffraction data [24], which corroborates the proposed reactions.

The corrosion current densities, determined from the polarization curves using the extrapolation method (Figure 6), increase with increase in both concentration and temperature. The variation of nat.log (corrosion current density) with the reciprocal temperature (T^{-1}) is nearly linear, which indicates the thermally activated character of the processes occurring at the Ta surface in NaOH solutions. The activation energy obtained from the slope of the curves, using Arrhenius' law, is in the 50–70 kJ mol^{-1} range. This range is of the same order as that obtained by Gad-Allah [18]. This author found two activation energies, 88.1 and 38.4 kJ mol^{-1} for dissolution of anodized tantalum in 3 M NaOH solutions, due to the duplex structure of the anodically grown oxide film.

The current densities measured in the passive region at 0.5 V vs SCE (i_{pass}) increase with increasing NaOH concentration and temperature and the critical current densities (i_{crit}), measured at the anodic current density maximum, for 30 wt % NaOH also increase with temperature (Figure 7).

The corrosion rates of Ta in NaOH solutions were calculated from the corrosion current densities using Faraday's law, assuming that Ta corrosion occurs with five-electron transfer (Table 2). Ta only presents a good corrosion resistance in very limited NaOH concentration/temperature conditions.

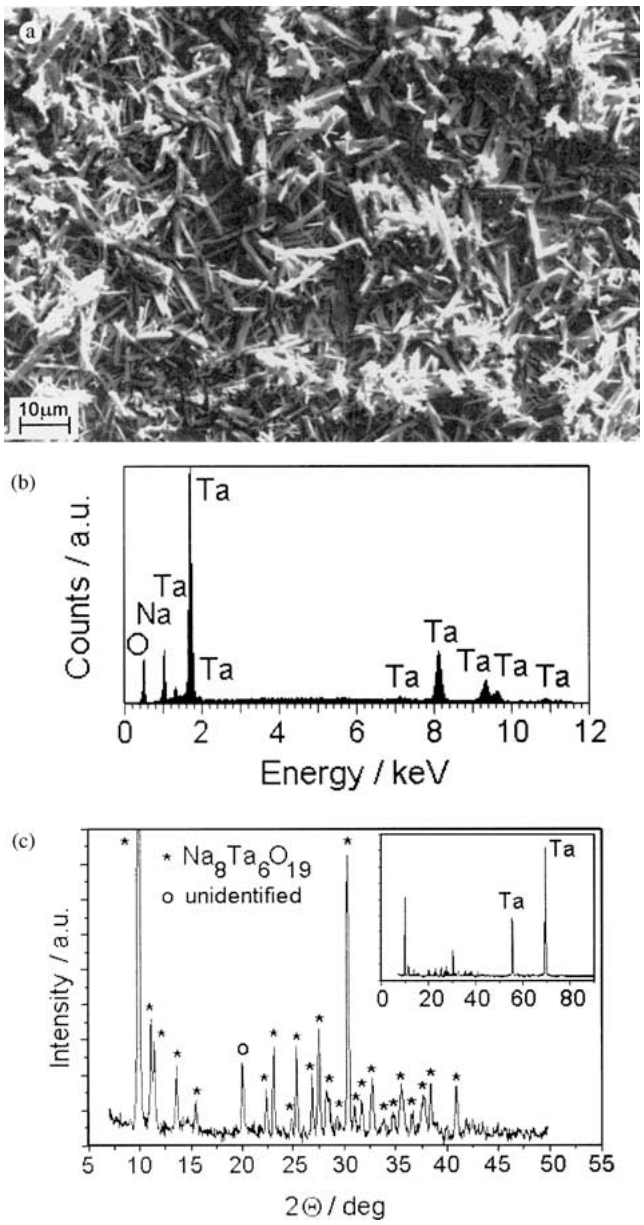

Fig. 5. (a) SEM photograph of Ta surface after immersion in 30 wt % NaOH at 25 °C for 54 h; (b) EDS spectrum of Ta surface; (c) X-ray diffraction pattern of Ta surface.

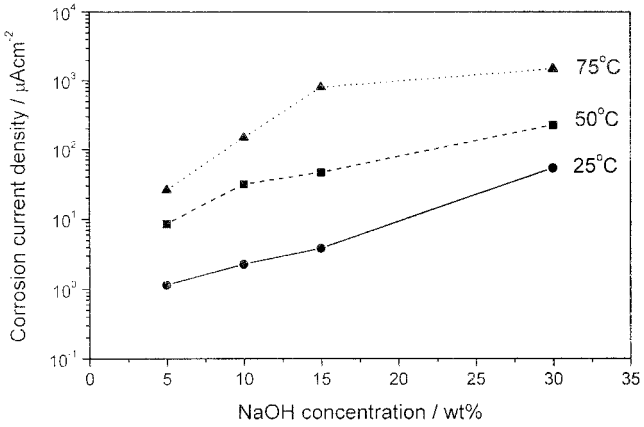

Fig. 6. Corrosion current densities of Ta in NaOH solutions at different temperatures.

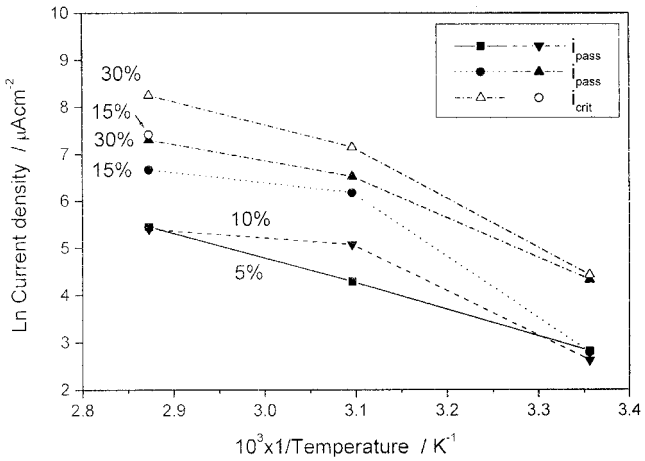

Fig. 7. Dependence of nat.log (passive current density) and nat.log (critical current density) on reciprocal temperature for Ta in NaOH solutions.

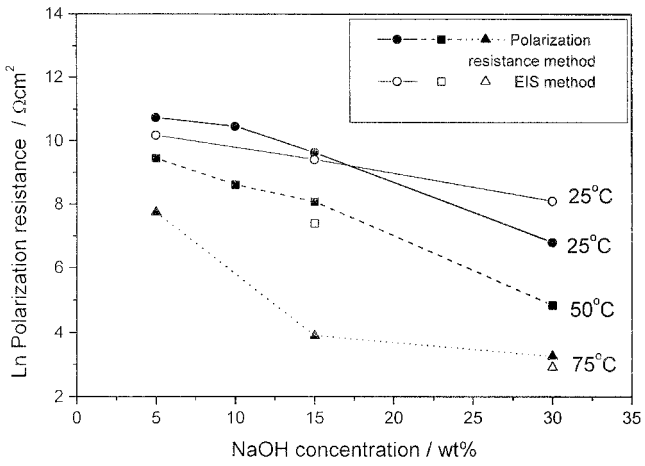

Fig. 8. Polarization resistance values of Ta as a function of NaOH concentration and temperature. Filled symbols (● ■ ▲) polarization resistance method; open symbols (○ □ △) EIS method.

Table 2. Corrosion rates (in μm y^{-1}) of Ta in NaOH solutions

Temperature /°C	NaOH concentration/wt %			
	5	10	15	30
25	8	16	27	380
50	61	222	328	1613
75	184	1054	5700	10 540

The polarization resistance values were determined from the slope of the fitted straight lines i/E in the OCP ± 0.020 V range as a function of NaOH concentration and temperature (Figure 8). As temperature and NaOH concentration increase, the polarization resistance decreases, showing an increase in corrosion rate.

EIS experiments were also carried out at OCP for different NaOH concentrations and temperatures. Figure 9 shows the results of impedance measurements obtained in 30 wt % NaOH at 25 °C, which were plotted on both Nyquist and Bode diagrams. Similar plots were obtained for the other investigated conditions (5 and 15 wt % NaOH at 25 °C, 15 wt % NaOH at 50 °C and 30 wt % NaOH at 75 °C). The Nyquist diagrams present depressed semicircles and the Bode diagrams show a linear relation between log |impedance| and log (frequency) and a phase angle close to 90° for the intermediate frequencies. This is characteristic of a predominantly capacitive behaviour. Badawy [14–16] obtained good results representing the electrode–electrolyte interface for Ta in aqueous solutions by the simple Randles equivalent circuit. This circuit consists of a

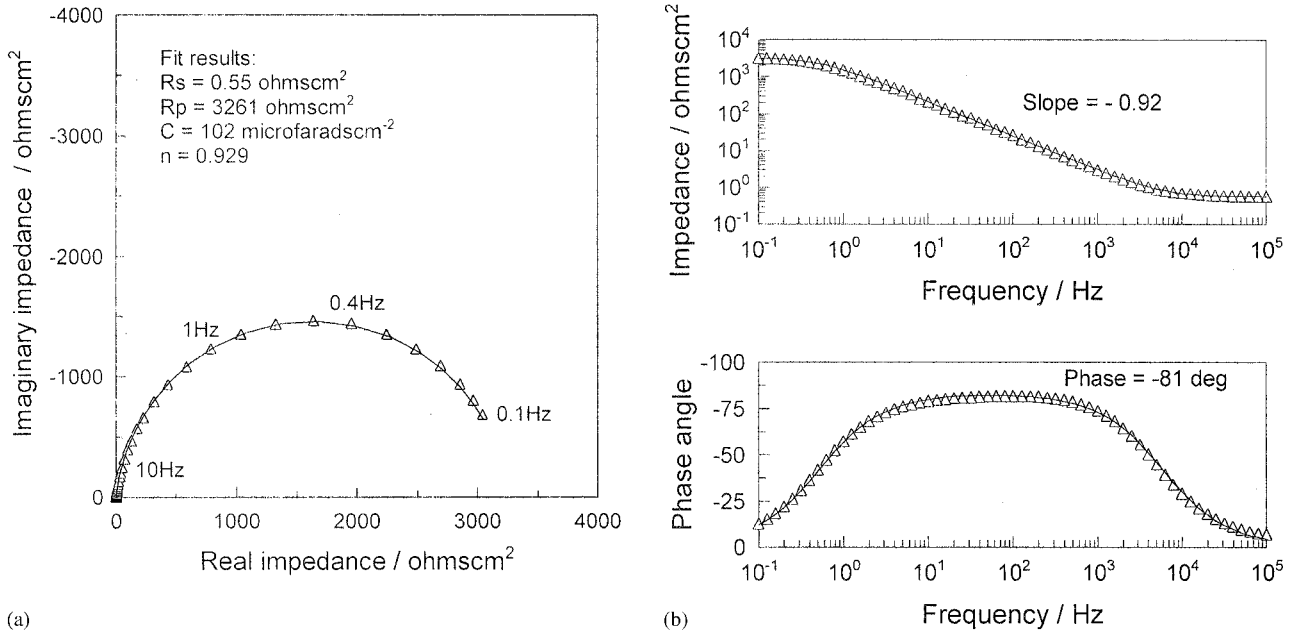

Fig. 9. Nyquist (a) and Bode (b) plots for Ta at OCP (−1.408 V vs SCE) in 30 wt % NaOH at 25 °C (Δ experimental data; — theoretical values calculated using the CPE model). Fit results in (a): $R_s = 0.55\ \Omega\ cm^2$, $R_p = 3261\ \Omega\ cm^2$, $C = \mu F\ cm^{-2}$ and $n = 0.929$.

capacitor parallel to a resistor and the solution resistance is simulated by a series resistor. In our case, the interface is better described by a circuit consisting of a constant-phase element (CPE) with a parallel resistor, and a series resistor to represent the electrolyte resistance. Such a model was shown to be suitable for this type of study [17, 25, 26]. The impedance of the CPE is defined as

$$Z_{\mathrm{CPE}} = \frac{1}{(i\omega)^n C} \tag{7}$$

with the value of n being related to a nonuniform current distribution due to surface roughness or non-homogeneity. Figure 9 shows that this model fits our experimental data quite well for Ta in NaOH solutions at OCP. The CPE parameter n and the phase angle deduced from the impedance data using this model are in the 0.90 to 0.93° and −80 to −82° ranges, respectively, which indicates that the interface does not behave as an ideal capacitor ($n = 1$ and phase angle −90°), in agreement with the need to use CPE as a model for the system. The polarization resistance extrapolated from the Nyquist diagrams to the Z values corresponding to the lowest frequency is reported in Figure 8. The values obtained by EIS (alternate current) are of the same order of magnitude as those obtained by the polarization resistance method (direct current).

The capacitance values of Ta at OCP, obtained from the fitting of our experimental data with the CPE/resistor model, are quite different when Ta is covered with the porous $Na_8Ta_6O_{19}$ corrosion product (active state) or covered with the Ta_2O_5 oxide film (passive state). In 30 wt % NaOH at 25 and 75 °C after self-activation of Ta, the capacitance values are 102 and 126 μF cm^{-2}, respectively. In 5 and 15 wt % NaOH at 25 °C and in 15 wt % NaOH at 50 °C, where Ta is passive, the measured capacitances were 32, 27 and 26 μF cm^{-2}, respectively. Considering that the oxide thickness (d) is related to the oxide capacitance (C)by the relation:

$$d = \frac{\varepsilon.\varepsilon_{\mathrm{o}}}{C} \tag{8}$$

where ε is the dielectric constant of Ta_2O_5 which is equal to 27.6 [27] and ε_{o} the permittivity of free space, 8.85×10^{-14} F cm^{-2}, the thickness of the spontaneous oxide film formed on Ta for these NaOH solutions and temperatures is in the 0.7 to 0.9 nm range. This thickness is of the same order as that obtained by Badawy [15] for passive Ta at OCP in 1 M HNO_3 at 25 °C.

4. Conclusions

Ta shows passive behaviour in 5 and 10 wt % NaOH at 25, 50 and 75 °C, and in 15 wt % NaOH at 25 and 50 °C. The surface is covered by the Ta_2O_5 oxide.

In 15 wt % NaOH at 75 °C and in 30 wt % NaOH at 25, 50 and 75 °C, Ta presents a passive–active transition (self-activation), due to the spontaneous dissolution of its superficial air-formed oxide and remains in the active state. The corrosion product was shown to be $Na_8Ta_6O_{19}$ polytantalate.

The corrosion current density, passive current density and critical current density (the latter for Ta in the active state) increase with increasing NaOH concentration and temperature.

Ta can be used in NaOH solutions only in very limited concentration/temperature conditions due to its high corrosion rates.

References

1. ASM Handbook, Vol. 13, Corrosion. ASM International, Metals Park, (1993) p. 725.
2. D. Lupton, W. Schiffmann, F. Schreiber and E. Heitz. Corrosion behaviour of tantalum and possible substitutes materials under extreme conditions, *in* Proceedings of the 8th International Congress on 'Metallic Corrosion', Vol. 2, Mainz (1981), p. 1441.
3. P. Eichner, A. Ferat, H. Mazille and C. Tamagne, Reactivité du tantale en milieu acide concentré et chaud: corrosion et fragilisation, *in* P. Barret and L.C. Dufour (Eds), 'Reactivity of Metals' (Elsevier Science, Amsterdam, 1985), p. 201.
4. A. Robin, *Int. J. Refr. Met. & Hard Mater.* **15** (1997) 317.
5. M. Coscia and M.H.W. Renner, *Mater. Perform.* January (1998) 52.
6. C. Friedrich, P. Kritzer, N. Boukis, G. Franz and E. Dinjus, *J. Mater. Sci.* **34** (1999) 3137.
7. A. Robin and J.L. Rosa, *Int. J. Refr. Met. & Hard Mater.* **18** (2000) 13.
8. F.J. Hunkeler, Properties of tantalum for applications in the chemical process industry, *in* R.E. Smallwood (Ed.), 'ASTM Special Technical Publication 849', ASTM (1984), p. 28.
9. R.H. Burns, F.S. Shuker and P.E. Manning. Industrial applications of corrosion resistant tantalum, niobium and their alloys, *in* R.E. Smallwood (Ed.), 'ASTM Special Technical Publication 849', ASTM (1984), p. 50.
10. C.E.D. Rowe, *Metal Constr.* **16** (1984) 68.
11. V. Macagno and J.W. Schultze, *J. Electroanal Chem.* **180** (1984) 157.
12. I. Uehara, T. Sakai, H. Ishikawa, E. Ishii and M. Nakane, *Corrosion* **42** (1986) 492.
13. I. Uehara, T. Sakai, H. Ishikawa, E. Ishii and H. Takenaka, *Corrosion* **45** (1989) 548.
14. W.A. Badawy, S.S. Elegamy and Kh.M. Ismail, *Br. Corr. J.* **28** (1993) 133.
15. W.A. Badawy and Kh.M. Ismail, *Electrochim. Acta* **38** (1993) 2231.
16. F.M. Al-Kharafi and W.A. Badawy, *Electrochim. Acta* **40** (1995) 2623.
17. G.E. Cavigliasso, M.J. Esplandiu and V.A. Macagno, *J. Appl. Electrochem.* **28** (1998) 1213.
18. A.G. Gad-Allah, W.A. Badawy and H.H. Rehan, *J. Appl. Electrochem.* **19** (1989) 768.
19. A.G. Gad-Allah, *J. Appl. Electrochem.* **21** (1991) 346.
20. N.M. Koshevnikova and A.L. Rotinyan, *J. Appl. Chem. USSR* **36** (1963) 1892.
21. M. Pourbaix, 'Atlas of Electrochemical Equilibria in Aqueous Solutions', Vol. 1 (Pergamon, New York, 1966), p. 253.
22. I.M. Gibalo, 'Analytical Chemistry of Niobium and Tantalum' (Ann Arbor–Humphrey Science Publishers, London, 1970), p. 30.
23. W.A. Badawy, A.G. Gad-Allah and H.H. Rehan, *J. Appl. Electrochem.* **17** (1987) 559.
24. Powder Diffraction Files – Inorganic Phases, JCPDS International Centre for Diffraction Data, Swarthmore (1988).
25. J.R. MacDonald, *J. Electroanal. Chem.* **223** (1987) 25.
26. M.J. Esplandiu, E.M. Patrito and V.A. Macagno, *Electrochim. Acta* **40** (1995) 809.
27. L. Young, *Proc. Royal. Soc. A.* **244** (1958) 41.